

# Studies on the Intermolecular Structural Heterogeneity of a Propylene-Ethylene Random Copolymer Using Preparative Temperature Rising Elution Fractionation

Yonggang Liu, Shuqin Bo, Yejuan Zhu, Wenhe Zhang

State Key Laboratory of Polymer Physics and Chemistry, Changchun Institute of Applied Chemistry, Chinese Academy of Sciences, Changchun 130022, People's Republic of China

Received 18 August 2003; accepted 9 December 2004

DOI 10.1002/app.21761

Published online in Wiley InterScience (www.interscience.wiley.com).

**ABSTRACT:** The intermolecular structural heterogeneity of a propylene-ethylene random copolymer was studied by preparative temperature rising elution fractionation combined with GPC,  $^{13}\text{C}$ -NMR, differential scanning calorimetry, and wide-angle X-ray diffraction analysis of the obtained fractions. The isotacticity of fractions increased with increasing elution temperature, and the ethylene content decreased monotonously. Fitting of the obtained comonomer triad sequences by Bernoullian and first-order Mark-

ovian statistical models indicated that lower isospecific active sites are more active toward ethylene. The isolated ethylene unit disrupted the crystallizable isotactic sequence and lowered the crystallizability of the polypropylene chain. © 2005 Wiley Periodicals, Inc. *J Appl Polym Sci* 97: 232–239, 2005

**Key words:** polypropylene; copolymer; temperature rising elution fractionation (TREF); GPC;  $^{13}\text{C}$ -NMR

## INTRODUCTION

The morphology, crystallinity, processability, and final properties of polyolefin copolymers are dependent on its molecular chain structure, which have heterogeneity in molecular weight, comonomer composition, and sequence distribution. Propylene-ethylene random copolymer, which contains a range of copolymers with different molecular weight distribution and composition distribution, is the case in point. Understanding the intermolecular structural heterogeneity of propylene-ethylene random copolymer is necessary to elucidate the relationship between its microstructure and properties.

Many analytical techniques have been employed to measure the structural heterogeneity of polyolefins. Temperature rising elution fractionation (TREF), a technique that fractionates semicrystalline polymers according to their solubility-temperature relationship, has been widely used for the characterization of compositional heterogeneity of polyolefins.<sup>1–3</sup> Gel permeation chromatography (GPC) has long been used to determine the molecular weight and molecular weight distribution of polymers.  $^{13}\text{C}$  nuclear magnetic resonance spectroscopy ( $^{13}\text{C}$ -NMR) has been used to study the comonomer composition and sequence distribution of polyolefin copolymers.<sup>4</sup>

In the present article we report on the intermolecular structural heterogeneity of a propylene-ethylene random copolymer characterized using preparative TREF combined with GPC and  $^{13}\text{C}$ -NMR analysis of the obtained fractions. The TREF-GPC cross-fractionation technique provided detailed information on the intermolecular structural heterogeneity of the studied copolymer. The thermal behaviors of TREF fractions were studied by differential scanning calorimetry (DSC). The crystallinity of TREF fractions was determined by DSC, as well as wide-angle X-ray diffraction (WAXD).

## EXPERIMENTAL

### Preparative temperature rising elution fractionation

The commercial propylene-ethylene random copolymer resin used in this study, namely PPR-Y, was produced by heterogeneous Ziegler–Natta catalyst and was kindly provided by China Petrochemical Corp. The isotacticity was  $[\text{mm}] = 95.1\%$  with ethylene content of 5.1 mol %, which was determined by  $^{13}\text{C}$ -NMR. The preparative TREF equipment used in this work has been described before.<sup>5</sup> About 8 g of polymer was dissolved in 600 mL of 1,2,4-trimethylbenzene (TMB) at 140°C.  $1 \times 10^{-3}$  g/mL 2,6-di-*tert*-butyl-4-methylphenol (BHT) was added to TMB as antioxidant. The polymer solution was introduced to the column packed with 60 ~ 80 mesh glass beads at 140°C, and the column was slowly cooled to room temperature in 80 h. The fractionation procedure then

Correspondence to: S. Bo (sqbo@ns.ciac.jl.cn).

TABLE I  
TREF and Molecular Weight Data

Fraction	Elution temperature (°C)	Weight (g)	$w_i$ (%)	$\Sigma w_i$ (%)	$M_w$ (k)	$M_n$ (k)	$M_w/M_n$
PPR-Y					574	123	4.67
Y1	40	0.7089	8.95	8.95	315	53.2	5.91
Y2	60	0.1669	2.11	11.06	126	42.6	2.96
Y3	80	0.4844	6.12	17.18	265	65.6	4.04
Y4	90	0.6086	7.69	24.87	318	78.0	4.07
Y5	95	0.4447	5.62	30.48	316	112	2.82
Y6	100	1.2584	15.89	46.38	380	146	2.59
Y7	118	4.2124	53.21	99.58	717	254	2.82
Y8	121	0.0082	0.10	99.69	—	—	—
Y9	140	0.0248	0.31	100.00	1369	653	2.10
Summation					537	129	4.17

was performed by increasing the temperature stepwise. Extraction took place over temperatures ranging from 40 to 140°C divided into 9 steps (40, 60, 80, 90, 95, 100, 118, 121, and 140°C). During each step, the column content was allowed to equilibrate at the set temperature overnight before it was eluted with 1200 mL of TMB. The eluted solution was cooled, precipitated with twice the volume of acetone, and filtered. The obtained polymer fractions were then dried in a vacuum oven at room temperature to constant weight.

### Characterization of TREF fractions

The molecular weight and molecular weight distribution (MWD) of PPR-Y and its TREF fractions were determined at 150°C by a PL-GPC 220 high temperature gel permeation chromatography (Polymer Laboratories Ltd.). The columns used were three PLgel 10- $\mu$ m mixed-B LS columns (300  $\times$  7.5 mm). The eluent was 1,2,4-trichlorobenzene stabilized with 5

$\times 10^{-4}$  g/mL BHT and was filtered with a 0.2  $\mu$ m pore size membrane before use. The injection volume was 200  $\mu$ L, and the flow rate was 1.0 mL/min.

$^{13}$ C-NMR were measured at 140°C on a Varian Unity 400 MHz Spectrometer. Polymer sample solutions were made by dissolving 70 ~ 75 mg of polymer in 0.5 mL of deuterated *o*-dichlorobenzene.

DSC scans were recorded on a Perkin-Elmer DSC-7 calorimeter. The samples (about 6 mg) were first heated from 50 to 200°C at a rate of 10°C/min, held at 200°C for 3 min to remove thermal history, then cooled from 200 to 50°C at 10°C/min, held at 50°C for 1 min, and finally heated again to 200°C at 10°C/min. Temperature calibration was performed using indium. Crystallization temperature  $T_c$ , heat of crystallization  $\Delta H_c$ , melting temperature  $T_m$ , and heat of fusion  $\Delta H_m$  were measured during cooling and reheating experiments, respectively.

The calorimetric crystallinity  $W_{c,h}$  was calculated from

$$W_{c,h} = \frac{\Delta H_m}{\Delta H_m^0} \quad (1)$$

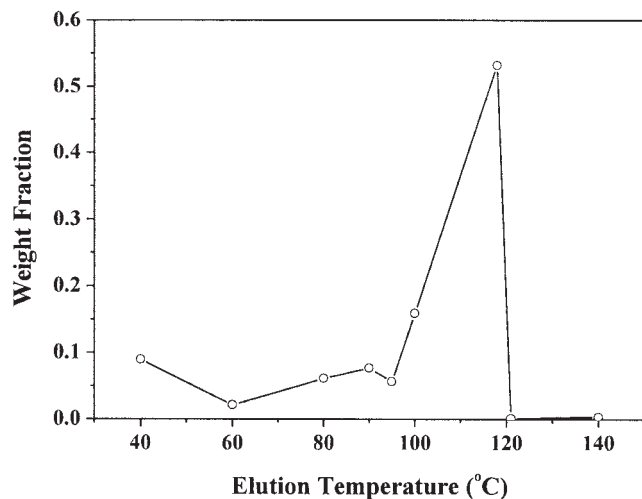


Figure 1 Weight fraction as a function of elution temperature for PPR-Y.

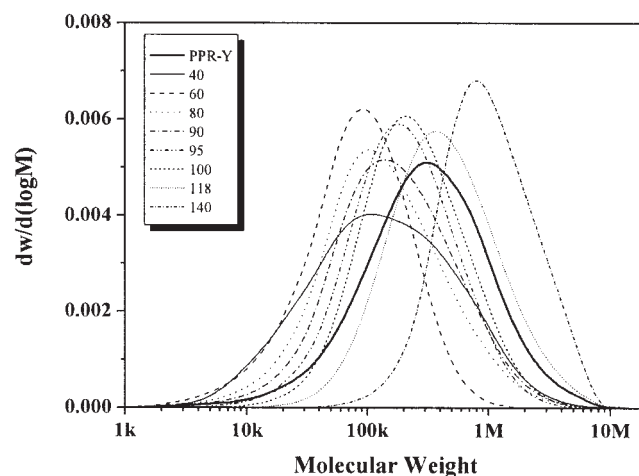


Figure 2 MWD profiles of PPR-Y and its TREF fractions.

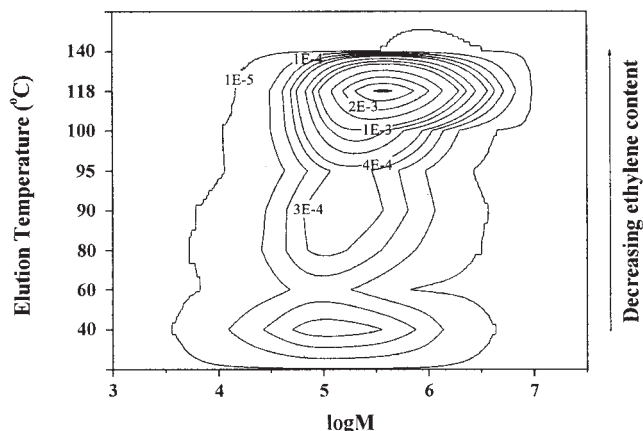


Figure 3 Contour plot of TREF-GPC analysis of PPR-Y.

where  $\Delta H_m$  is the heat of fusion of a semicrystalline PP and  $\Delta H_m^0$  is that of a 100% crystalline PP sample.  $W_{c,h}$  was calculated by assuming  $\Delta H_m^0 = 138 \text{ J/g}$ .<sup>6</sup>

WAXD experiments were carried out on powered samples at ambient temperature using a Rigaku D/max 2500V PC X-ray diffractometer. Nickel-filtered  $\text{Cu K}\alpha_1$  X-rays with wavelength of 0.154056 nm generated at 40 kV and 200 mA were employed. Scattered intensities were measured as a function of  $2\theta$  values between 5 and  $50^\circ$  in steps of  $0.02^\circ$ .

The X-ray crystallinity  $W_{c,x}$  was calculated from

$$W_{c,x} = \frac{I_c}{I_c + KI_a} \quad (2)$$

where  $I_c$  represents the integrated area of crystalline diffraction peaks,  $I_a$  is a corresponding portion of the amorphous halo, and  $K$  is a correction factor.  $W_{c,x}$  was calculated by assuming  $K = 1$ .

## RESULTS AND DISCUSSION

### Intermolecular structural heterogeneity of PPR-Y

The total recovery of TREF fractionation was 99.0%, and 9 fractions were obtained. The fractionation data are summarized in Table I. The weight fraction as a function of elution temperature is shown in Figure 1. It can be seen that PPR-Y was eluted over a broad temperature range, indicating much heterogeneity in both isotacticity and composition for this propylene-ethylene random copolymer.

The MWD curves of PPR-Y and its TREF fractions are profiled in Figure 2. The molecular weight data are also listed in Table I. The molecular weight of the fractions tended to increase with increasing elution temperature, except Y1, the fraction eluted at  $40^\circ\text{C}$ . However, it is not to say the fractionation was based on molecular weight. The fraction eluted at  $40^\circ\text{C}$  had a much more broader MWD than the other fractions,

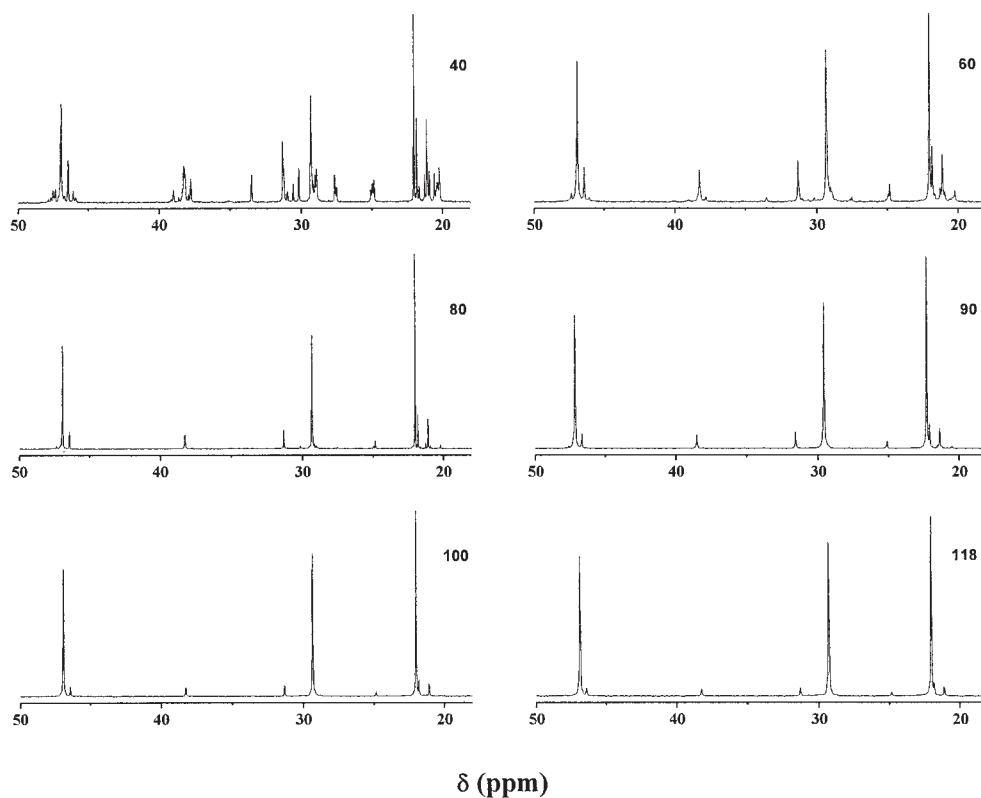


Figure 4  $^{13}\text{C}$ -NMR spectra of TREF fractions of PPR-Y.

**TABLE II**  
Monomer and Configurational Composition  
for Some Fractions

Fraction	P (mol %)	E (mol %)	mm (%)	mr (%)	rr (%)
PPR-Y	94.9	5.1	95.1	2.6	2.3
Y1	78.0	22.0	65.3	7.4	27.3
Y2	88.8	11.2	85.0	8.0	7.0
Y3	93.0	7.0	95.3	3.5	1.2
Y4	95.2	4.8	96.4	2.5	1.1
Y6	97.0	3.0	98.2	1.3	0.5
Y7	97.9	2.1	99.4	0.4	0.2

since it simultaneously contained components with low molecular weight and components with low stereo regularity and higher molecular weight.

A TREF-GPC cross-fractionation contour plot was constructed for PPR-Y, as shown in Figure 3. As we will discuss below, the isotacticity of copolymer increased and ethylene content decreased monotonously with increasing elution temperature. Thus, each region on the plot gives the relative amount of the species with a given molecular weight and composition. The resolution is somewhat poorer than that obtained from Mitsubishi cross-fractionation chromatography because only 8 fractions were taken here.<sup>7,8</sup> However, it still illustrated the great heterogeneity in both composition and molecular weight for PPR-Y. It can be seen that PPR-Y was composed of a series of components with different composition and molecular weight, which were produced by multiple active sites of the heterogeneous Ziegler-Natta catalyst.

<sup>13</sup>C-NMR spectra of the TREF fractions are shown in Figure 4. The intensity of each peak in the <sup>13</sup>C-NMR spectra was used to calculate the comonomer composition and sequence distribution. It should be

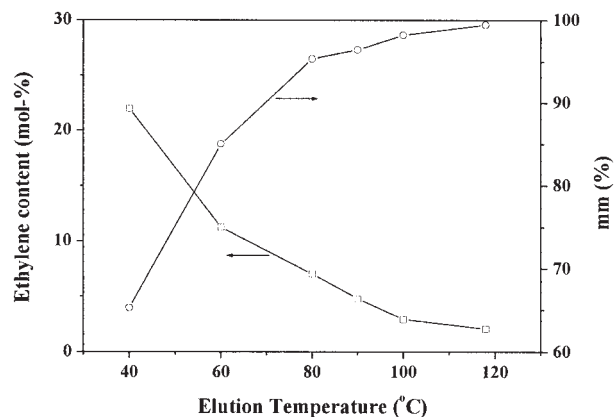


**Figure 5** Ethylene content and isotactic triad fraction as functions of elution temperature for PPR-Y.

noted that the resonance associated with propylene unit tail-to-tail arrangement,  $S_{\alpha\beta}$ , was not observed in the spectra of all fractions. Thus, the methyl resonance can be used to calculate the configurational triad sequence distributions of propylene (mm, mr, and rr) after subtracting the respective overlapped propylene-centered compositional triad sequence arrangements.<sup>9</sup>

The monomer content and configurational sequence distribution for some fractions are summarized in Table II. As elution temperature increased from 40 to 118°C, the isotactic triad fraction (mm) increased from 65.3% to 99.4%, while the ethylene content decreased from 22.0 mol % to 2.1 mol % (Fig. 5). It indicated that the studied propylene-ethylene copolymer contained a range of copolymers with different composition, which were produced by different active sites with different selectivity to ethylene and propylene and

**TABLE III**  
Compositional Triad Sequence Distribution for Some Fractions

Fraction		EEE	EEP	PEP	EPE	PPE	PPP	SS × 10 <sup>4</sup>
Y1	Observed	0.038	0.073	0.109	0.054	0.211	0.515	
	Bernoullian	0.007	0.061	0.126	0.030	0.252	0.524	37.0
	Markovian	0.020	0.090	0.102	0.027	0.239	0.522	22.1
Y2	Observed	0.012	0.024	0.076	0.017	0.149	0.722	
	Bernoullian	0.001	0.018	0.081	0.009	0.162	0.729	4.64
	Markovian	0.003	0.028	0.074	0.009	0.160	0.726	3.06
Y3	Observed	0.009	0.007	0.054	0.008	0.115	0.807	
	Bernoullian	0.000	0.009	0.059	0.004	0.118	0.810	1.34
	Markovian	0.001	0.011	0.058	0.004	0.118	0.808	1.27
Y4	Observed	0.002	0.005	0.041	0.005	0.088	0.859	
	Bernoullian	0.000	0.005	0.044	0.002	0.089	0.860	0.24
	Markovian	0.000	0.006	0.043	0.002	0.089	0.859	0.18
Y6	Observed	0.000	0.002	0.028	0.002	0.063	0.905	
	Bernoullian	0.000	0.002	0.031	0.001	0.062	0.904	0.11
	Markovian	0.000	0.003	0.030	0.001	0.062	0.904	0.11
Y7	Observed	0.000	0.000	0.021	0.000	0.049	0.930	
	Bernoullian	0.000	0.001	0.022	0.001	0.044	0.932	0.31
	Markovian	0.000	0.001	0.022	0.000	0.044	0.933	0.31

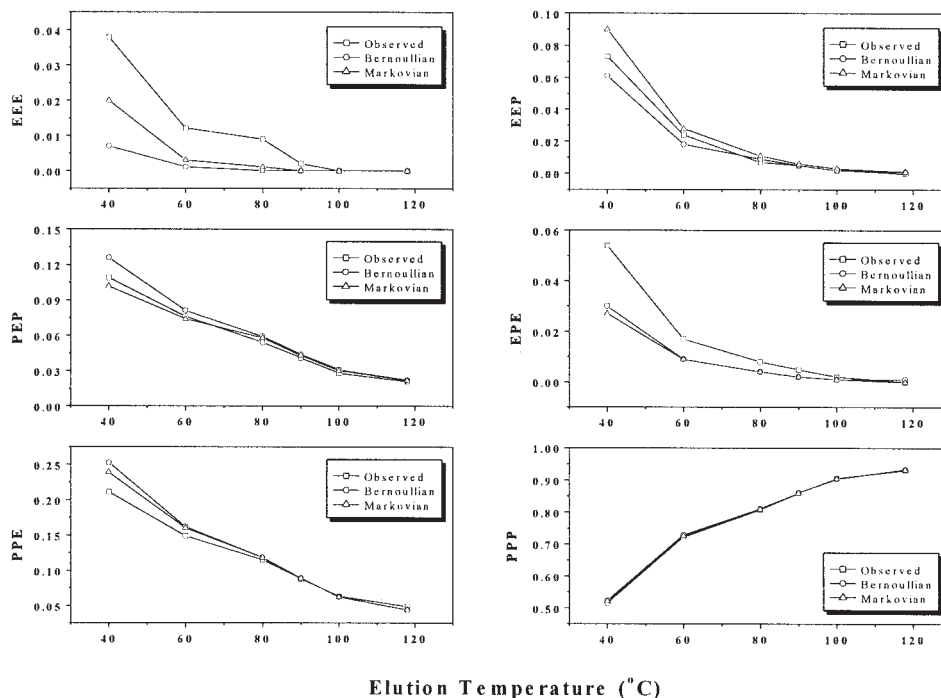


**Figure 6** Observed and calculated compositional triad sequence distribution as functions of elution temperature for PPR-Y.

that more ethylene inserted into the chains with lower stereo regularity during copolymerization. The ethylene units insert into the chain and shorten the isotactic sequence as the other structural defects, such as stereo defects and regio errors in isotactic polypropylene. Thus the fractionation is based on isotacticity and isotactic sequence length, which control the crystallizability of the chain. Further analysis of  $^{13}\text{C}$ -NMR data will give direct proof. Kakugo and colleagues had studied an ethylene-propylene copolymer containing 0.41 mol %  $^{13}\text{C}$ -enriched ethylene by TREF and also found that lower isospecific active centers are more active toward ethylene.<sup>10</sup>

The compositional triad sequence distribution is shown in Table III. The fractions were mainly composed of long propylene sequences with an occasional ethylene unit, such as PPE and PEP. Further analysis of triad distribution with Bernoullian and first-order Markovian statistical models gave information on ethylene distribution in the copolymer. Calculated triad distributions, obtained from best fits based on both Bernoullian and first-order Markovian statistics, are given in Table III and shown in Figure 6. The extent of fitting to a certain model is evaluated by the sum of squares of the deviation ( $SS$ ).<sup>11</sup> It had been suggested that  $SS$  less than  $10 \times 10^{-4}$  is an indication that a given model adequately represents the copolymerization process. A comparison of calculated triad sequence distributions favors the first-order Markovian model. However, for the fraction eluted at  $40^\circ\text{C}$ ,  $SS$  was a little

higher for both the Bernoullian and first-order Markovian models, indicating a two-site or even three-site model should be used, as a result of multiple active sites and thus much heterogeneity in this fraction, which agreed with the much broader MWD of the fraction.

The differences between the first-order Markovian conditional probabilities  $P_{EE}$ ,  $P_{PE}$ , and  $P_{PP}$ ,  $P_{EP}$ , as given in Table IV, is another evidence for first-order Markovian behavior of these propylene-ethylene copolymers. As shown in Figure 7, the conditional probabilities with the order  $P_{PP} > P_{EP} \gg P_{EE} > P_{PE}$  indicated that a long propylene sequence is favored. In addition, as elution temperature increased, the probability for chain propagation with ethylene ( $P_{EE}$ ,  $P_{PE}$ ) decreased, indicating that lower isospecific active sites are more active toward ethylene, which confirmed the above conclusion. The values of the reactivity ratio

**TABLE IV**  
First-Order Markovian Conditional Probabilities  
on Best Fit for Some Fractions

Fraction	$P_{EE}$	$P_{PE}$	$P_{PP}$	$P_{EP}$	$r_E r_P$
Y1	0.306	0.186	0.814	0.694	1.93
Y2	0.160	0.099	0.901	0.840	1.73
Y3	0.086	0.068	0.932	0.914	1.29
Y4	0.069	0.049	0.951	0.931	1.44
Y6	0.043	0.033	0.967	0.957	1.32
Y7	0.030	0.023	0.977	0.970	1.31



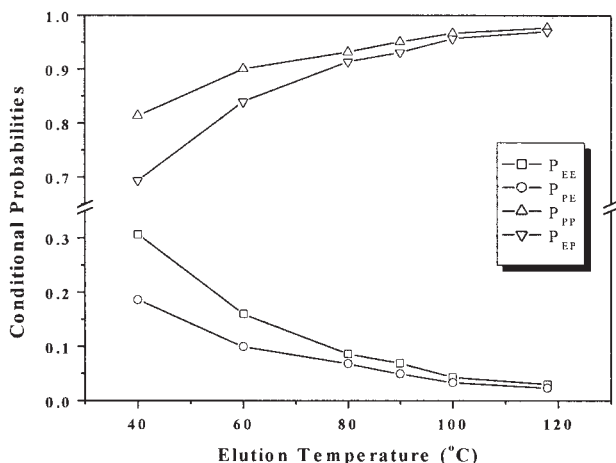


**Figure 7** First-order Markovian conditional probabilities on best fit as functions of elution temperature for PPR-Y.

product  $r_{EP}$ , which were calculated from the conditional probabilities, were close to unity, as expected for an ideal random copolymerization, as shown in Table IV.

The number-average sequence length of the comonomer blocks was calculated, and the results are listed in Table V. The comonomer blocks calculated from Bernoullian and first-order Markovian statistics were also included. As elution temperature increased, the length of P-blocks increased, indicating TREF fractionated propylene-ethylene copolymer according to the longest crystallizable sequence of chains. The length of E-blocks is very short (less than 1.5) in all fractions, indicating that ethylene inserts into the chain in isolated units and acts as a structural defect of the isotactic polypropylene chain.

The ethylene content of PPR-Y is profiled as a function of  $M_w$  in Figure 8. It can be seen that ethylene content decreased with increasing  $M_w$  except for Y1, the fraction eluted at 40°C. It explained the increase of molecular weights of the fractions with elution temperature. Different authors had also observed decreasing of ethylene content with increasing molecular weight for propylene-ethylene random copoly-

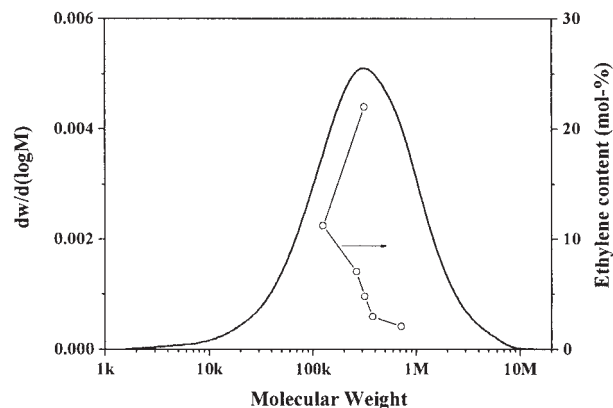


**Figure 8** Ethylene content as a function of  $M_w$  for PPR-Y.

mer.<sup>10,12</sup> The fraction eluted at 40°C contained components with low molecular weight and components with higher molecular weight and high ethylene content (low stereo regularity); it had a high ethylene content and much broader MWD.

#### Thermal behaviors and crystallinity

Table VI summarizes the values of  $T_c$ ,  $T_m$ ,  $\Delta H_c$ ,  $\Delta H_m$ ,  $W_{c,w}$  and  $W_{c,x}$  for TREF fractions of PPR-Y. As shown in Figure 9, both  $T_c$  and  $T_m$  decreased with increasing ethylene content. It suggested that the isolated ethylene units disrupted the crystallizable isotactic sequence and lowered the crystallizability of the polypropylene chain. Consequently,  $\Delta H_c$  and  $\Delta H_m$  also decreased with increasing ethylene content.

As shown in Figure 10, the WAXD diffractographs of TREF fractions of PPR-Y exhibited characteristic peaks of  $\alpha$ -PP and no polyethylene crystalline peak was observed, indicating that the ethylene sequence was not sufficiently long to crystallize. It suggested that ethylene units inserted into the random copolymer chain in isolated units, which agreed with the above <sup>13</sup>C-NMR results. It should also be noted that more ethylene inserted into the chain of fraction obtained at lower elution temperature, resulting in a larger amorphous halo from more amorphous component.

**TABLE V**  
Number-Average Sequence Length of Comonomer Blocks for Some Fractions

Fraction	Measured values		Bernoullian		Markovian	
	$n_E$	$n_P$	$n_E$	$n_P$	$n_E$	$n_P$
Y1	1.49	5.06	1.24	5.15	1.44	5.38
Y2	1.27	9.89	1.11	10.11	1.19	10.10
Y3	1.20	15.00	1.07	14.71	1.09	14.71
Y4	1.10	20.63	1.05	20.41	1.07	20.41
Y6	1.03	31.07	1.03	30.30	1.04	30.30
Y7	1.00	43.40	1.02	43.48	1.03	43.48

TABLE VI  
 $T_c$ ,  $T_m$ ,  $\Delta H_c$ ,  $\Delta H_m$ ,  $W_{c,h}$  and  $W_{c,x}$  for Some Fractions

Fraction	$T_c$ (°C)	$T_m$ (°C)	$\Delta H_c$ (J/g)	$\Delta H_m$ (J/g)	$W_{c,h}$ (%)	$W_{c,x}$ (%)
Y1	42.2	83.4	10.7	3.89	2.82	21.5
Y2	58.8	99.8	35.3	28.7	20.8	39.5
Y3	80.5	120.1	53.4	52.6	38.1	47.3
Y4	92.9	133.4	62.7	68.0	49.3	54.1
Y5	97.1	138.2	67.9	76.3	55.3	60.2
Y6	101.2	142.6	77.7	76.2	55.3	60.2
Y7	103.2	147.2	80.8	86.3	62.6	62.6
Y9	108.8	148.2	82.9	80.2	58.1	—

Figure 11 shows that the crystallinity of the fractions as determined by DSC and WAXD increased with increasing elution temperature, confirming that the fractionation was based on crystallizability of the molecules. The components with higher ethylene content had lower crystallinity and eluted at lower temperature, while the fractions eluted at higher temperature had lower ethylene content and higher crystallinity. It should be noted that Y9, the fraction eluted at a higher temperature of 140°C, had lower crystallinity than Y8, the fraction eluted at a lower temperature of 118°C. However, Y9 had a higher  $T_c$  and  $T_m$  and thus a longer isotactic sequence. It was a result of the imperfection of crystallization due to restricted mobility of very long chains in this high molecular weight fraction, which had also been observed for isotactic polypropylene.<sup>5,13</sup>

### CONCLUSIONS

A propylene-ethylene random copolymer containing 5.1 mol % ethylene was fractionated by preparative TREF based on crystallizability of different chains in the copolymer. Further studies of the TREF fractions

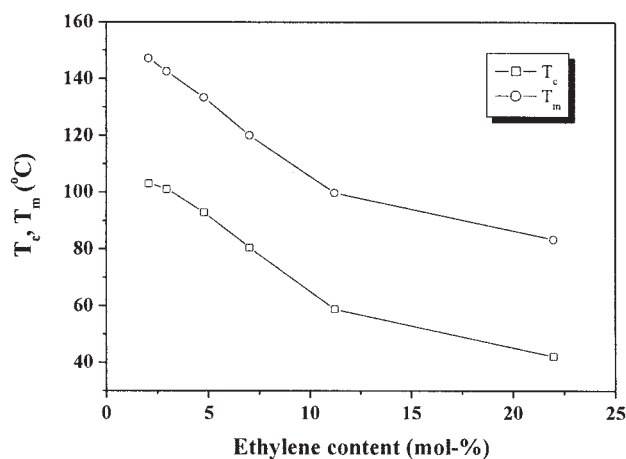


Figure 9  $T_c$  and  $T_m$  as functions of ethylene content for PPR-Y.

by GPC and  $^{13}\text{C}$ -NMR showed that the studied propylene-ethylene copolymer contained a range of copolymers with different composition and molecular weight distribution, which were produced by multiple active sites of the heterogeneous Ziegler-Natta catalyst.

The isotacticity of fractions increased with increasing elution temperature, and the ethylene content decreased monotonously, indicating that lower isospecific active sites are more active toward ethylene.

The isolated ethylene unit disrupted the crystallizable isotactic sequence and lowered the crystallizability of the polypropylene chain. The comonomer composition and sequence distribution in the copolymer had a great effect on its thermal behaviors and crystallinity.

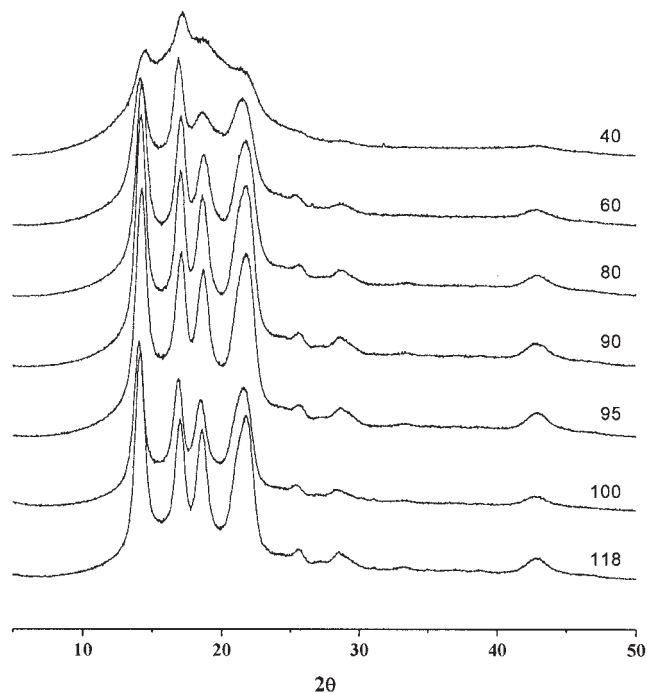
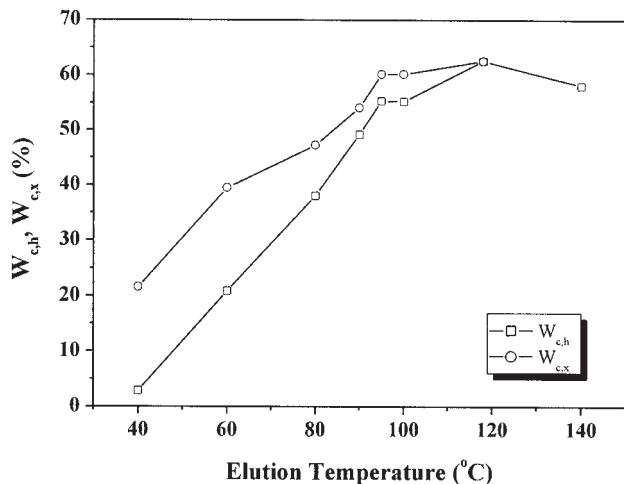


Figure 10 WAXD diffractograms of TREF fractions of PPR-Y.



**Figure 11**  $W_{c,h}$  and  $W_{c,x}$  as functions of elution temperature for PPR-Y.

This work was subsidized by the Special Funds for Major State Basic Research Projects of China and supported by the

State Key Laboratory of Polymer Physics and Chemistry of China.

## References

1. Soares, J. B. P.; Hamielec, A. E. *Polymer* 1995, 36, 1639.
2. Xu, J.; Feng, L. *Eur Polym J* 2000, 36, 867.
3. Feng, Y.; Hay, J. N. *Polymer* 1998, 39, 6589.
4. Ray, G. J.; Johnson, P. E.; Knox, J. R. *Macromolecules* 1977, 10, 773.
5. Liu, Y.; Bo, S. *Int J Polym Anal Charact* 2003, 8, 225.
6. Yuksekkalayci, C.; Yilmazer, U.; Orbey, N. *Polym Eng Sci* 1999, 39, 1216.
7. Usami, T.; Gotoh, Y.; Umemoto, H.; Takayama, S. *J. Appl Polym Sci: Appl Polym Symp* 1993, 52, 145.
8. Faldi, A.; Soares, J. B. P. *Polymer* 2001, 42, 3057.
9. Randall, J. C. *Polymer Sequence Determination: Carbon-13 NMR Method*; Academic Press: New York, 1977.
10. Kakugo, M.; Miyatake, T.; Mizunuma, K.; Kawai, Y. *Macromolecules* 1988, 21, 2309.
11. Cozewith, C. *Macromolecules* 1987, 20, 1237.
12. Verdurmen-Noël, L.; Baldo, L.; Bremmers, S. *Polymer* 2001, 42, 5523.
13. Viville, P.; Daoust, D.; Jonas, A. M.; Nysten, B.; Legras, R.; Dupire, M.; Michel, J.; Debras, G. *Polymer* 2001, 42, 1953.